Orbit Control for a Power Generating Airfoil Based on Nonlinear MPC

Sébastien Gros, Mario Zanon and Moritz Diehl

Abstract— **The Airborne Wind Energy paradigm proposes to generate energy by flying a tethered airfoil across the wind flow. An essential problem posed by Airborne Wind Energy is the control of the tethered airfoil trajectory during power generation. Tethered flight is a fast, strongly nonlinear, unstable and constrained process, motivating control approaches based on fast Nonlinear Model Predictive Control. In this paper, a computationally efficient 6-DOF control model for a high performance, large-scale, rigid airfoil is proposed. A control scheme based on receding-horizon Nonlinear Model Predictive Control to track reference trajectories is applied to the proposed model. In order to make a real-time application of Nonlinear Model Predictive Control possible, a Real-Time Iteration scheme is proposed and its performance investigated.**

Keywords **: flight control, fast NMPC, trajectory tracking, Real-time iteration, Optimal Control**

I. INTRODUCTION

To overcome the major difficulties posed by the exponentially growing size and mass of conventional wind turbine generators [14], [2], the Airborne Wind Energy (AWE) paradigm proposes to get rid of the structural elements not directly involved in power generation. An emerging consensus recognizes crosswind flight as the most efficient approach to perform power generation [15]. Crosswind flight essentially consists in extracting power from the airflow by flying an airfoil tethered to the ground at a high velocity across the wind direction. Power can be generated by (a) performing a cyclical variation of the tether length, together with cyclical variation of the tether tension or (b) by using on-board turbines, transmitting the power to the ground via the tether. In this paper, option (a) is considered.

Because it involves a much lighter structure, a major advantage of power generation based on crosswind flight over conventional wind turbines is that higher altitude can be reached and a larger swept area can arguably be achieved, hence reaching wind resources that cannot be tapped into by conventional wind turbines.

While the potential efficiency of the principle is established in theory, a major research effort is still required to address the many engineering difficulties posed by its implementation. Among the several issues that have been identified so far, the control of tethered flight is a major challenge. The control problems currently recognized as most crucial are a) control during power generation b) control during airfoil retrieval and c) control during airfoil launch. This paper addresses the problem of control during power generation.

S. Gros, M. Zanon and M. Diehl are with the Optimization in Engineering Center (OPTEC), K.U. Leuven, Kasteelpark Arenberg 10, B-3001 Leuven-Heverlee, Belgium. sgros@esat.kuleuven.be, mario.zanon@esat.kuleuven.be, moritz.diehl@esat.kuleuven.be

In [10], a reliable methodology for designing power generating periodic trajectories (i.e. orbits) is presented. Because the actuator limitations and process constraints are significantly activated by the resulting orbits and because the process dynamics are strongly nonlinear, this paper proposes to tackle tethered flight control through Nonlinear Model Predictive Control (NMPC).

Classical NMPC approaches suffer from two major drawbacks when applied to fast processes: a) the computational time required to compute input updates can be prohibitively large in a real-time scenario, and b) the latency between the computation of the process state estimation and the corresponding process inputs update can be large, hence imposing a significant delay between measurement and the resulting control actions.

Because tethered flight is a fast, unstable and perturbed process, both issues are critical for the applicability of the NMPC scheme to a real AWE system. To address these issues, the Real-Time Iteration (RTI) scheme has been proposed in [7], [13]. RTI proposes to reduce the computational time required by conventional NMPC scheme by performing a single Newton-type iteration per control input update instead of several SQP steps. Moreover, the RTI scheme proposes to reduce the control update latency by preparing most of the computations without a priori knowledge of the process state so as to perform the Newton-type step in a negligible time when the process state estimation becomes available.

In [6], a fast NMPC scheme based on RTI was successfully tested in simulation for the control of a rudimentary power generating kite model in the presence of perturbations of the process initial conditions. Recently, a simple model was shown to allow NMPC sampling time of 1 ms [9]. The model considered the kite as a point-mass, assuming a) a perfect control of the time derivative of the lift coefficient (C_{L}), b) a perfect control of the roll rate, c) that the side slip is perfectly cancelled by some ad-hoc control, and d) that the yaw rate is unbounded. Because these assumptions are not realistic in practice, a more elaborate control model is required.

This paper proposes a model that considers the airfoil as a rigid-body, 6-DOF object interacting with the air mass. It is assumed in this model that the pitch-roll-yaw acceleration rates are directly controlled, i.e. it is assumed that a fast inner-loop controller is efficiently tracking the pitch-roll-yaw rate references provided by the NMPC controller.

A NMPC scheme based on the proposed model and tracking a power generating trajectory is presented, resulting

in computational performance that is suitable for a real-time application. So as to propose a realistic scenario, the case study presented in the simulations considers a turbulent wind velocity as the process disturbance.

This paper is organized as follows. The process model is presented in Section II, the NMPC scheme is proposed in Section III. Simulation results are presented in Section IV. Future developments and conclusions are proposed in Section V.

Contribution of the paper: this paper proposes a 6-DOF model for tethered flight control, for which a NMPC control scheme based on the RTI technique is developed and tested in simulations in the presence of turbulent wind.

II. Process Model

The airfoil is considered as a rigid body having 6 degrees of freedom (DOF). An orthonormal reference frame $e = \{e_x, e_y, e_z\}$ attached to the ground is chosen to generate the Cartesian coordinate system defining the position of the airfoil center of mass. The frame e is chosen s.t. a) the wind is blowing in the e_x-direction, b) the vector e_z is opposed to the gravitational acceleration vector g, and c) vector e_y is defined by $e_y = e_z \times e_x$. The origin of the coordinate system coincides with the generator. Defining the set of coordinates $\{x,y,z\}$, the position of the airfoil center of mass is given by $\mathcal{P} = xe_x + ye_y + ze_z$. In the following, the coordinate vector $X \in \mathbb{R}^3$ is defined as $X := [x, y, z]^T$. The tether is approximated as a rigid link of (time-varying) length r that constrains X (i.e. the airfoil center of mass) to evolve on the 2-dimensional manifold $C = \frac{1}{2}\left(X^T X - r^2\right) = 0$. Such an assumption requires that the tether is always under tension. In this paper, it is assumed that the second time derivative of the tether length, i.e. $\ddot{r} \in \mathbb{R}$ is a control variable.

Spherical coordinates can appear as a more reasonable choice to describe the proposed system, yet the choice of Cartesian coordinates can be motivated by the following features:

- the computational complexity of the model equations in Cartesian coordinates is lower than in spherical coordinates
- a model based on cartesian coordinates is better suited for further model developments, i.e. for including a) tether dynamics, b) a tether attached to a moving point on the ground, used to transfer energy to the airfoil [8], and c) the modeling of dual (or multiple) airfoil systems

An orthonormal reference frame $\mathcal{E} = \{\mathcal{E}_x, \mathcal{E}_y, \mathcal{E}_z\}$ is attached to the airfoil s.t. a) the basis vector $\mathcal{E}_x$ spans the airfoil longitudinal axis, pointing in the forward direction and is aligned with the airfoil chord, b) the basis vector $\mathcal{E}_z$ spans the vertical axis, pointing in the upward direction, and c) the basis vector $\mathcal{E}_y$ is given by $\mathcal{E}_y = \mathcal{E}_z \times \mathcal{E}_x$. The origin of $\mathcal{E}$ is attached to the center of mass of the airfoil. The description of the airfoil attitude is given by the operator performing the change of reference frame $\mathcal{E} \to e'$, where e' is a translation of e to the airfoil center of mass. In order to avoid model singularities resulting from a representation based on Euler angles, quaternions are preferred [17]. The change of reference frame $\mathcal{E} \to e'$ is obtained by the rotation matrix R:

$$
\begin{aligned}
&R = EG^T,\\
&G = \begin{bmatrix} -q_1 & q_0 & q_3 & -q_2 \\ -q_2 & -q_3 & q_0 & q_1 \\ -q_3 & q_2 & -q_1 & q_0 \end{bmatrix},\\
&E = \begin{bmatrix} -q_1 & q_0 & -q_3 & q_2 \\ -q_2 & q_3 & q_0 & -q_1 \\ -q_3 & -q_2 & q_1 & q_0 \end{bmatrix}.
\end{aligned} \tag{1}
$$

Because the set of coordinates $\{x,y,z\}$ describes the position of the center of mass of the airfoil, the translational dynamics and the rotational dynamics are separable. It is assumed in the proposed formulation that the airfoil pitch-roll-yaw accelerations are directly controlled, i.e. defining ω as the projection of the airfoil angular velocity vector in the airfoil frame $\mathcal{E}$, the airfoil rotational dynamics reduce to:

$$
\dot{q} = \frac{1}{2} G^T \omega, \quad \dot{\omega} = T, \quad \left(q^T q\right)_{t=0} = 1, \tag{2}
$$

where $T \in \mathbb{R}^3$ is a set of control variables. Because $q^T \dot{q} = 0$, the quaternion norm constraint $q^T q = 1$ is preserved by the dynamics (2). Yet, for long integration times, a correction of the numerical drift of the quaternion norm may be needed.

The kinetic and potential energy functions associated to the translational dynamics of the airfoil read:

$$
\mathcal{T}_\mathrm{A} = \tfrac{1}{2} F_\mathrm{A} \dot{X}^T \dot{X}, \quad \mathcal{V}_\mathrm{A} = F_\mathrm{A} g z,
$$

where F_A is the mass of the airfoil. The kinetic and potential energy functions associated to the translational dynamics of the tether read:

$$
\mathcal{T}_\mathrm{T} = \tfrac{1}{2} \int_0^1 \sigma^2 \dot{X}^T \dot{X} \mu r d\sigma = \tfrac{1}{6} \mu r \dot{X}^T \dot{X}, \quad \mathcal{V}_\mathrm{T} = \tfrac{1}{2} \mu r g z,
$$

where μ is the tether linear density. The Lagrangian associated to the translational dynamics of the system reads:

$$
\mathcal{L} = \mathcal{T}_\mathrm{A} + \mathcal{T}_\mathrm{T} - \mathcal{V}_\mathrm{A} - \mathcal{V}_\mathrm{T} + \lambda C,
$$

where λ is the Lagrange multiplier associated to the algebraic constraint C. With $\mathcal{V} = \mathcal{V}_\mathrm{A} + \mathcal{V}_\mathrm{T}$, using the Lagrange equation

$$
\frac{d}{dt}\frac{\partial \mathcal{L}}{\partial \dot{X}} - \frac{\partial \mathcal{L}}{\partial X} = F,
$$

the system translational dynamics are given by the following index-3 DAE:

$$
m\ddot{X} + \dot{m}\dot{X} + \mathcal{V}_X = F + \lambda X, \quad C = 0, \tag{3}
$$

where $\mathcal{V}_X^T = \nabla_X \mathcal{V} = \begin{bmatrix} 0 & 0 & \left(F_\mathrm{A} + \frac{1}{2}\mu r\right) g \end{bmatrix}$, F is the coordinate vector of generalized forces associated to $\{x,y,z\}$ and $m = F_\mathrm{A} + \frac{1}{3}\mu r$.

As an alternative to using (3), an index-reduction allows to reformulate (3) as a set of ODEs. For any $t_0 \in \mathbb{R}$, using $\ddot{C}(t) = 0, \dot{C}(t_0) = 0, C(t_0) = 0$, the resulting index reduction

of (3) yields the index-1 DAE (together with the consistency conditions):

$$\begin{aligned} M\begin{bmatrix} \ddot{X} \\ \lambda \end{bmatrix} &= \begin{bmatrix} F - \mathcal{V}_X - \dot{m}\dot{X} \\ \dot{X}^T\dot{X} - \dot{r}^2 - r\ddot{r} \end{bmatrix}, \qquad (4) \\ M &= \begin{bmatrix} m\cdot I_3 & -X \\ -X^T & 0 \end{bmatrix}, \\ 2C(t_0) &= \left(X^TX - r^2\right)_{t=t_0} = 0, \\ \dot{C}(t_0) &= \left(X^T\dot{X} - r\dot{r}\right)_{t=t_0} = 0, \end{aligned}$$

where I_3 is the 3×3 identity matrix. Because the algebraic state λ appears linearly in (4), the accelerations $\ddot{X}$ and the Lagrange multiplier λ are given by:

$$\begin{aligned} \begin{bmatrix} \ddot{X} \\ \lambda \end{bmatrix} &= M^{-1}\begin{bmatrix} F - \mathcal{V}_X - \dot{m}\dot{X} \\ \dot{X}^T\dot{X} - \dot{r}^2 - r\ddot{r} \end{bmatrix}, \qquad (5) \\ M^{-1} &= \frac{1}{X^TX}\begin{bmatrix} \frac{1}{m}\left(X^TXI_3 - XX^T\right) & -X \\ -X^T & -m \end{bmatrix}, \end{aligned}$$

hence the translational dynamics can be treated as a set of ODEs. Similarly to (2), a correction of the numerical drift of C may be required for long integration times. The force in the tether is readily given by

$$F_\mathrm{T} = \|\lambda X\| = \lambda r. \qquad (6)$$

Because a Cartesian coordinate system is used, the generalized forces F in (4) are given by the sum of the aerodynamic forces acting at the airfoil center of mass, projected in frame e. Introducing the relative velocity v, i.e. the velocity of the airfoil w.r.t the air mass given by:

$$v = (\dot{x} - W)\,e_x + \dot{y}e_y + \dot{z}e_z\,,$$

where $W \in \mathcal{W} \in \mathbb{R}$ is the local wind velocity field projected in frame e, the norms of the lift and drag forces are given by [17]:

$$\|F_\mathrm{L}\| = \frac{1}{2}\rho A C_\mathrm{L}\|v\|^2, \qquad \|F_\mathrm{D}\| = \frac{1}{2}\rho A C_\mathrm{D}\|v\|^2,$$

where C_L and C_D are the lift and drag coefficient respectively, ρ is the air density and A the airfoil surface.

The lift force is orthogonal to the relative velocity v. Moreover, it is assumed in this model that the lift force is orthogonal to the airfoil transversal axis spanned by E_y, therefore the lift force is collinear to the vector L given by:

$$L = v \times E_y.$$

Note that L is normed to $\|v\|$. The drag force is defined as collinear and opposed to the relative velocity v. The lift and drag forces, F_L and F_D acting on the airfoil are therefore given by:

$$F_\mathrm{L} = \frac{1}{2}\rho A C_\mathrm{L}\|v\|L, \qquad F_\mathrm{D} = -\frac{1}{2}\rho A C_\mathrm{D}\|v\|v.$$

In order to compute the lift and drag forces in frame e, vectors E_y and v shall be projected in e. These projections are given by:

$$[E_y]_e = R\cdot\mathbf{1}_y, \quad [v]_e = \begin{bmatrix} \dot{x} - W & \dot{y} & \dot{z} \end{bmatrix}^T,$$

where R is given by (1) and $\mathbf{1}_y = [E_y]_\mathcal{E} = \begin{bmatrix} 0 & 1 & 0 \end{bmatrix}^T$. The resulting total aerodynamic force in the ground frame e, i.e. $F_\mathrm{A} = [F_\mathrm{L} + F_\mathrm{D}]_e$ is:

$$\begin{aligned} F_\mathrm{A} &= \frac{1}{2}\rho A\left(C_\mathrm{L}\,[v]_e \times R\cdot\mathbf{1}_y - C_\mathrm{D}\,[v]_e\right)\|v\|, \\ \|v\| &= \left((\dot{x} - W)^2 + \dot{y}^2 + \dot{z}^2\right)^{\frac{1}{2}}. \end{aligned}$$

In this model, it is assumed that the lift and drag coefficients C_L and C_D depend on the angle of attack α and side-slip angle β only. For some range $\alpha_\mathrm{min} \le \alpha \le \alpha_\mathrm{max}$ and $-\beta_\mathrm{max} \le \beta \le \beta_\mathrm{max}$, C_L and C_D are well approximated by [17], [4]:

$$\begin{aligned} C_\mathrm{L} &= C_\mathrm{L}^\alpha\alpha, \\ C_\mathrm{D} &= C_\mathrm{D}^0 + C_\mathrm{D}^I(C_\mathrm{L})^2 + C_\mathrm{D}^\beta\beta^2, \end{aligned}$$

where C_D^0, C_D^I and C_D^β are the airfoil drag, the induced drag, and the side slip drag coefficients respectively, while C_L^α is the lift coefficient slope. The proposed quadratic dependence of C_L on β arises from the symmetry of the system and a Taylor expansion of the drag coefficient with respect to β; note that [17] neglects this contribution, while [4] proposes a linear dependence w.r.t. $|\beta|$.

Defining $v = [v_x, v_y, v_z]^T$ as the coordinate vector of the relative velocity v projected in the airfoil frame $\mathcal{E}$, i.e.:

$$v = [v]_\mathcal{E} = R^T\,[v]_e\,,$$

for small angles α and β can be approximated by [17]:

$$\begin{aligned} \alpha &= -\tan^{-1}\left(\frac{v_z}{v_x}\right) \approx -\frac{v_z}{v_x}, \\ \beta &= \tan^{-1}\left(\frac{v_y}{\left(v_x^2 + v_z^2\right)^{\frac{1}{2}}}\right) \approx \frac{v_y}{\left(v_x^2 + v_z^2\right)^{\frac{1}{2}}}. \end{aligned}$$

Assuming a laminar wind flow with a logarithmic wind shear model blowing in the uniform e_x-direction, W is given by [16]:

$$W(z) = W_0\frac{\log(z/z_\mathrm{r})}{\log(z_0/z_\mathrm{r})},$$

where $W_0 \in \mathbb{R}$ is the wind velocity at altitude z_0 and z_r is the ground roughness. For the sake of simplicity, in this paper only the wind along the x-axis is considered. A generalization of this formulation to a 3D wind field is straightforward.

In this paper, the approximate tether drag model proposed in [11] is used. The tether drag is lumped into a single equivalent force F_T^D (projected in frame e) acting at the airfoil center of mass (see [11]) given by :

$$F_\mathrm{T}^D = -\frac{1}{8}\rho D_\mathrm{T}C_\mathrm{T}r\|\,[v]_e - \dot{r}e_r\|\left([v]_e - \dot{r}e_r\right),$$

where $e_r = r^{-1}\begin{bmatrix} x, & y, & z \end{bmatrix}^T$, D_T is the tether diameter, and C_T the tether drag coefficient. The sum of the forces F in (5) acting at the airfoil center of mass is given by $F = F_\mathrm{A} + F_\mathrm{T}^D$. Using (6), the generated energy is readily given by $\dot{E} = -\dot{r}\,F_\mathrm{T}$.

The following boundary conditions are required for the consistency of the model dynamics:

$$\begin{aligned} \left(X^T X - r^2\right)_{t=t_0} &= 0, \qquad \left(X^T \dot{X} - r\dot{r}\right)_{t=t_0} = 0, \\ \left(q^T q - 1\right)_{t=t_0} &= 0. \end{aligned} \tag{7}$$

In the following, the process dynamics and the process boundary conditions (7) will be put in the form:

$$\dot{\mathcal{X}} = f\left(\mathcal{X}, \mathcal{U}, W_0\right), \quad g\left(\mathcal{X}(t_0)\right) = 0,$$

where f lumps together the process dynamics described in this section, $\mathcal{U} = [\ddot{r}, T_1, T_2, T_3]^T \in \mathbb{R}^4$ are the process control input, and $\mathcal{X} = [x, y, z, \dot{x}, \dot{y}, \dot{z}, q_0, q_1, q_2, q_3, \omega_1, \omega_2, \omega_3, r, \dot{r}]^T \in \mathbb{R}^{15}$ are the process state trajectories.

A. Summary of the process model assumptions and limitations

Assumptions

The proposed model is based on the following assumptions:

1) tether elasticity and dynamics are neglected, the tether drag is approximated using a linear wind shear model, the tether is always under tension
2) direct control of the Roll/Pitch/Yaw accelerations
3) lift force is orthogonal to the airfoil transversal axis
4) lift and drag coefficients depend on the angle of attack α and the side-slip angle β only
5) angle of attack α and side-slip angle β are small
6) linear-lift model, quadratic drag model

Limitations

The proposed model is singular for the degenerate scenarios a) $X = 0$ (airfoil collapses to the origin) and b) $v_x = 0$ (airfoil longitudinal speed drops to zero). Moreover, the wind shear model prohibits $z \leq z_\mathrm{r}$ (airfoil very close to the ground).

B. Process Constraints

We propose the following control input bounds:

$$\begin{aligned} -40\,\mathrm{deg/s^2} &\leq T_k \leq 40\,\mathrm{deg/s^2}, \quad k = 1,2,3 \\ -5\,\mathrm{m/s^2} &\leq \ddot{r} \leq 5\,\mathrm{m/s^2}, \end{aligned} \tag{8}$$

and the following path constraints:

$$\begin{aligned} -40\,\mathrm{deg/s} &\leq \omega_k \leq 40\,\mathrm{deg/s}, \quad k = 1,2,3 \\ -10\,\mathrm{m/s} &\leq \dot{r} \leq 10\,\mathrm{m/s}. \end{aligned} \tag{9}$$

In the following, (8) and (9) are lumped together as the inequality constraints $h\left(\mathcal{X}, \mathcal{U}\right) \leq 0$.

In addition, in order to keep the process in the region where the model assumptions are valid, the following path constraints need to be considered:

$$\begin{aligned} 0 \leq C_\mathrm{L}\left(\mathcal{X}, W_0\right) &\leq 1, \\ \lambda\left(\mathcal{X}, W_0\right) &\leq 0. \end{aligned} \tag{10}$$

Constraint $\lambda \leq 0$ is required to keep the tether under tension (model Assumption 1), and constraint $0 \leq C_\mathrm{L} \leq 1$ is required to keep the airfoil in the linear-lift region [17] (model Assumption 6). Note that the actual bounds on the linear-lift region depend on the airfoil used.

III. NMPC Algorithm

A. NMPC Formulation

It is proposed here to formulate a receding horizon NMPC scheme using a least squares (LSQ) function penalizing the deviation of the process control input and states from the periodic power-generating reference trajectories. Because a small side-slip angle β is crucial for the process performance and for an efficient trajectory tracking, a penalty on β is introduced in the NMPC cost function.

The inequality constraints $0 \leq C_\mathrm{L} \leq 1$ and $\lambda \leq 0$ in (10) are pure state constraints and are directly affected by the wind velocity W_0, therefore wind turbulences can drive the process trajectories out of the feasible domain. This is especially a problem for the constraint $C_\mathrm{L} \leq 1$ which is active at the power-generation reference trajectories. To tackle this issue, the following slack reformulation of constraints (10) is proposed:

$$C_\mathrm{L} - S_1 \leq 1, \quad C_\mathrm{L} + S_1 \geq 0, \quad \lambda - S_2 \leq 0, \quad S_{1,2} \geq 0,$$

and a L_1 penalty on the slack variables S_k is included in the NMPC cost function. In the presence of process disturbances, violations of the original constraints $0 \leq C_\mathrm{L} \leq 1$ and $\lambda \leq 0$ cannot be excluded. Thus some robustness w.r.t. violations of constraints (10) need to be considered in the system design, e.g. the airfoil shall be designed such that a transition to a stall situation (C_L becomes too large) occurs smoothly and can be easily recovered from [4].

The NMPC is based on repeatedly ($i = 0, 1, \ldots$) solving the following optimal control problem (OCP):

$$\begin{aligned} \min_{\mathcal{U}_i(.), S} \quad & W_S S + \int_{t_i}^{t_i + T_\mathrm{H}} \left(\|\mathcal{X} - \bar{\mathcal{X}}\|_Q^2 + \|\mathcal{U}_i - \bar{\mathcal{U}}\|_R^2 \right. \\ & \qquad \left. + Q_\beta \beta^2 \right) dt, \\ s.t. \quad & \dot{\mathcal{X}} = f\left(\mathcal{X}, \mathcal{U}, W_0\right), \quad h\left(\mathcal{X}, \mathcal{U}, W_0\right) \leq 0, \\ & \mathcal{X}(t_i) = \hat{\mathcal{X}}\left(t_i\right), \qquad W_0 = \hat{W}_0\left(t_i\right), \qquad S \geq 0, \\ & C_\mathrm{L} - S_1 \leq 1, \quad C_\mathrm{L} + S_1 \geq 0, \quad \lambda - S_2 \leq 0, \end{aligned} \tag{11}$$

where $t_i = i T_\mathrm{s}$ and T_s is the NMPC sampling time, T_H the NMPC prediction horizon, $\bar{\mathcal{X}}\left(t + T_o\right) = \bar{\mathcal{X}}\left(t\right)$ and $\bar{\mathcal{U}}\left(t + T_o\right) = \bar{\mathcal{U}}\left(t\right)$, $\forall t \in \mathbb{R}$ are the state and input reference trajectories computed off-line, $\bar{C}_\mathrm{L}(\cdot) = C_\mathrm{L}\left(\bar{\mathcal{X}}, \bar{\mathcal{U}}, W_0\right)$ is the corresponding reference trajectory for the lift coefficient, Q and R are constant positive-definite weighting matrices, Q_{C_L} and Q_β are positive constant weights. Vector $S = \begin{bmatrix} S_1 & S_2 \end{bmatrix}^T$ is the set of slack variables, and $W_S \geq 0$ the corresponding row vector of positive weights. Vectors $\hat{\mathcal{X}}(t_i)$ and $\hat{W}_0\left(t_i\right)$ are the estimated process state and wind velocity at time instant t_i.

Note that the process state estimate must satisfy the consistency condition $g\left(\hat{\mathcal{X}}(t_i)\right) = 0$.

The methodology used to compute the power generating reference orbits is similar to the one presented in [11]. For the sake of brevity the details are omitted in this paper.

B. NMPC Implementation

Approximate solutions to OCP (11) are computed using the software package *ACADO* [12]. A piecewise-constant

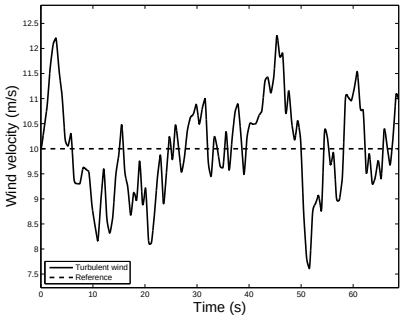

Fig. 1. Perturbed wind velocity W_0 (plain line) and reference wind velocity (dashed line), in (m/s).

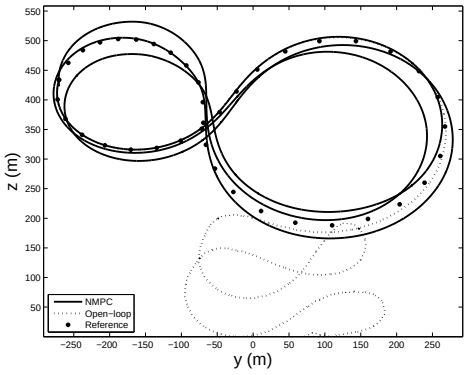

Fig. 2. Simulated trajectories for the airfoil *y*-*z* position: NMPC trajectories (plain line), open-loop trajectories (dotted line) and reference trajectories (the dots are the points on the multiple-shooting grid), in (m).

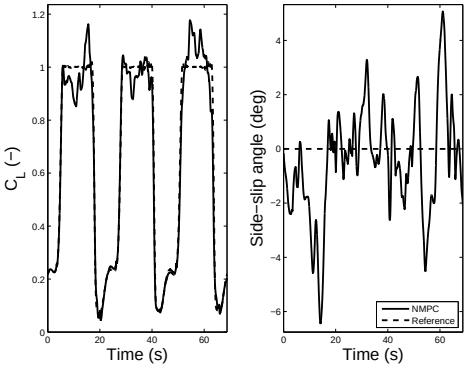

Fig. 3. *Left*: Simulated trajectory for the lift coefficient (C_L) and reference C_L (dashed line). *Right*: simulated trajectory for the side-slip angle (β) (plain line) and reference (dashed line), in (deg).

control vector parametrization (CVP) of the process control input $\mathcal{U}(.)$ is used. The chosen NMPC prediction horizon was set to $T_\mathrm{H} = T_\mathrm{o}/2$, where $T_\mathrm{o} = 22.94\,\mathrm{s}$. The CVP is based on $N = 20$ elements of uniform duration $T_\mathrm{cvp} = T_\mathrm{H}/N$. The OCP is discretized using a multiple-shooting method [1], using the CVP time grid. The process dynamics f are discretized over the shooting intervals via the Runge-Kutta 45 integration method. The NMPC sampling time $T_\mathrm{s} = t_i - t_{i-1}$ was chosen as $T_\mathrm{s} = T_\mathrm{cvp}$. Matrix Q was chosen diagonal, with:

$$\begin{aligned}\mathrm{diag}\{Q\} = \quad & 10^{-4} \cdot [3.6,\ 0.08,\ 0.22,\ 5,\ 5,\ 5,\\ & 10,\ 10,\ 10,\ 10,\ 10,\ 10,\ 10,\ 0,\ 1].\end{aligned}$$

The remaining weights in (11) were chosen as $\mathrm{diag}\{R\} = \left[4 \cdot 10^{-4}, 20, 20, 20\right]$, $W_S = \begin{bmatrix} 10^2 & 10^2 \end{bmatrix}$, and $Q_\beta = 10^3$. Note that the units of the weights are defined consistently with the variables they correspond to, so as to yield a dimensionless cost.

A real-time implementation of the NMPC scheme requires that the time needed to provide a solution to the NLP approximating (11) is consistently less than T_s. The NLP was repeatedly solved via the RTI method where a) at each sampling time t_i the control inputs are updated using a single Newton step instead of several SQP iterations, resulting in approximate but faster control input updates, and b) most of the linear algebra involved in the QP providing the control input update is prepared without knowledge of the future process state and parameter estimation, resulting in a negligible control latency. See [7], [13], [6] for a detailed description of the RTI scheme.

IV. Simulation results

In this Section, the simulation results obtained for the model proposed in Section II and the control algorithm proposed in Section III are presented. The model parameters are summarized in Table I. The proposed scenario considers a turbulent wind velocity as the process disturbance. Standard turbulent wind models for wind energy are available in the literature [3], yet for sake of simplicity a simple perturbation of $W_0 = 10\,\mathrm{m/s}$ was considered in this paper, based on a Gaussian random walk smoothened by a first-order filter. The perturbed wind velocity profile is displayed in Fig. 1.

In order to clearly distinguish the control problem from the state estimation problem, it is assumed here that exact knowledge of the process state is available. However, because the estimation of the local wind velocity for AWE systems is still a fully open question, it was assumed here that no estimation of the actual wind velocity is available, i.e. $\hat{W}_0(t_i) = W_0$ was used in the NMPC formulation.

The proposed simulation was run over the duration of three orbits. The *y*-*z* trajectory is presented in Fig. 2, alongside with the *y*-*z* reference trajectory on the multiple-shooting grid points. The lift coefficient C_L and side slip angle β are displayed in Fig. 3. The averaged power generation $\bar{P} = E/T_\mathrm{o}$ can be seen in Fig. 4.

The time required for the computation of the NMPC input updates was of the order of the NMPC sampling frequency T_s. It should be underlined here that this computational performance can be significantly improved via auto-generated C-code [9].

V. Conclusion & Further developments

This paper has proposed a computationally efficient 6-DOF control model dedicated to the control of tethered flight specific to the Airborne Wind Energy concept. The model is well suited for an integration into a NMPC scheme acting as a high-level controller providing pitch-roll-yaw reference trajectories to a lower-level controller. The proposed model

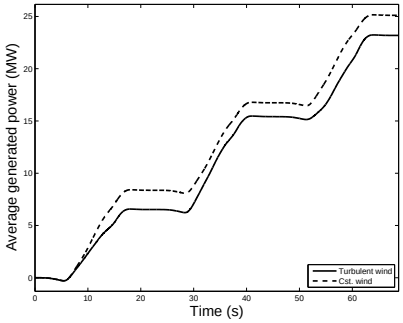

Fig. 4. Simulated trajectory of the averaged power generation (plain line), and averaged power generation without process perturbation (dashed line) in (MW).

TABLE I
MODEL PARAMETERS

Parameter	Value	Unit
m_{A}	$5 \cdot 10^3$	(kg)
A	500	(m^2)
C_{L}^{α}	5.67	-
C_{D}^{0}	10^{-2}	-
C_{D}^{I}	10^{-2}	-
C_{D}^{β}	10^{-1}	-
ρ	1.23	$(\mathrm{kg} \cdot \mathrm{m}^{-3})$
D_{T}	$5 \cdot 10^{-2}$	(m)
C_{T}	1	-
μ	2.84	$(\mathrm{kg} \cdot \mathrm{m}^{-1})$
z_{r}	10^{-2}	$(\mathrm{m} \cdot \mathrm{s}^{-1})$
z_0	100	(m)

was integrated into a fast NMPC algorithm based on the Real-Time Iteration scheme performing the tracking of a power-generating reference trajectory. The control scheme was successfully tested in simulation in the presence of a turbulent wind velocity.

A. Further developments

Tether dynamics have been neglected in this paper. However, for large scale AWE systems, the tether dynamics are likely to have a significant impact on the process behavior. The development of a computationally efficient tether dynamics model and the integration of such a model into the NMPC scheme are the object of current research.

The computational performance can significantly be improved via auto-generated C-code [9]. In addition, because multiple-shooting is an ideal framework for a parallelization of the highly time-consuming sensitivity evaluations, future research will consider the implementation of fast NMPC schemes for tethered flight on multi-core platforms, hence dividing the time required for the sensitivity evaluation by a corresponding factor.

The process performance is sensitive to process disturbances. It has been observed in simulations that a low side-slip angle β is crucial for both the trajectory tracking and the power generation. However, future research will consider a more formal approach to performance tracking, by e.g. casting the control problem in the framework of Economic MPC [5].

Finally, simulations based on state-of-the-art 3D turbulent flow models are the object of future research.

VI. ACKNOWLEDGMENTS

The research was supported by the Research Council KUL via GOA/11/05 Ambiorics, GOA/10/09 MaNet, CoE EF/05/006 Optimization in Engineering (OPTEC) en PFV/10/002 (OPTEC), IOF-SCORES4CHEM and PhD/postdoc/fellow grants, the Flemish Government via FWO (PhD/postdoc grants, projects G0226.06, G0321.06, G.0302.07, G.0320.08, G.0558.08, G.0557.08, G.0588.09, G.0377.09, research communities ICCoS, ANMMM, MLDM) and via IWT (PhD Grants, Eureka-Flite+, SBO LeCoPro, SBO Climaqs, SBO POM, O&O-Dsquare), the Belgian Federal Science Policy Office: IUAP P6/04 (DYSCO, Dynamical systems, control and optimization, 2007-2011), the IBBT, the EU (ERNSI; FP7-HD-MPC (INFSO-ICT-223854), COST intelliCIS, FP7-EMBOCON (ICT-248940), FP7-SADCO (MC ITN-264735), ERC HIGHWIND (259 166)), the Contract Research (AMINAL), the Helmholtz Gemeinschaft via viCERP and the ACCM.

REFERENCES

[1] H.G. Bock and K.J. Plitt. A multiple shooting algorithm for direct solution of optimal control problems. In *Proceedings 9th IFAC World Congress Budapest*, pages 243–247. Pergamon Press, 1984.

[2] E. A. Bossanyi. Further Load Reductions with Individual Pitch Control. *Wind Energy*, 8:481–485, 2005.

[3] Burton, T., Sharpe, D., Jenkins, N. and Bossanyi, E. *Wind Energy Handbook*. 2002.

[4] Michael V. Cook. *Flight Dynamics Principles*. Elsevier Science, 2007.

[5] M. Diehl, R. Amrit, and J.B. Rawlings. A Lyapunov Function for Economic Optimizing Model Predictive Control. *IEEE Trans. of Automatic Control*, 56(3):703–707, March 2011.

[6] M. Diehl, H.G. Bock, and J.P. Schlöder. A real-time iteration scheme for nonlinear optimization in optimal feedback control. *SIAM Journal on Control and Optimization*, 43(5):1714–1736, 2005.

[7] M. Diehl, H.G. Bock, J.P. Schlöder, R. Findeisen, Z. Nagy, and F. Allgöwer. Real-time optimization and Nonlinear Model Predictive Control of Processes governed by differential-algebraic equations. *J. Proc. Contr.*, 12(4):577–585, 2002.

[8] M. Diehl and B. Houska. Windenergienutzung mit schnell fliegenden Flugdrachen: eine Herausforderung für die Optimierung und Regelung - Wind Power via Fast Flying Kites: a Challenge for Optimization and Control. *at-automatisierungstechnik*, 57(10):525–533, 2009.

[9] H.J. Ferreau, B. Houska, K. Geebelen, and M. Diehl. Real-time control of a kite-carousel using an auto-generated nonlinear MPC algorithm. In *Proceedings of the IFAC World Congress*, 2011.

[10] B. Houska. Robustness and Stability Optimization of Open-Loop Controlled Power Generating Kites. Master's thesis, University of Heidelberg, 2007.

[11] B. Houska and M. Diehl. Optimal Control for Power Generating Kites. In *Proc. 9th European Control Conference*, pages 3560–3567, Kos, Greece,, 2007. (CD-ROM).

[12] B. Houska, H.J. Ferreau, and M. Diehl. ACADO Toolkit – An Open Source Framework for Automatic Control and Dynamic Optimization. *Optimal Control Applications and Methods*, 32(3):298–312, 2011.

[13] B. Houska, H.J. Ferreau, and M. Diehl. An Auto-Generated Real-Time Iteration Algorithm for Nonlinear MPC in the Microsecond Range. *Automatica*, 47(10):2279–2285, 2011.

[14] J.H. Laks, L.Y. Pao, and A.D. Wright. Control of Wind Turbines: Past, Present, and Future. In *American Control Conference*, pages 2096–2103, 2009.

[15] M.L. Loyd. Crosswind Kite Power. *Journal of Energy*, 4(3):106–111, July 1980.

[16] Manwell, J. F., McGowan, J. G. and Rogers, A. L. *Wind Energy Explained: Theory, Design and Application, Second Edition*. 2009.

[17] Pamadi. *Performance, Stability, Dynamics, and Control of Airplanes*. American Institute of Aeronautics and Astronautics, Inc., 2003.